


Research Article

Coal Facies and Its Effects on Pore Characteristics of the Late Permian Longtan Coal, Western Guizhou, China

Yi Lou,^{1,2} Yuliang Su ,¹ Wendong Wang,¹ Peng Xia ,³ Ke Wang,³ Wei Xiong,⁴ Yin Yu,³ Linjie Shao,² Fuqin Yang,² and Xiangping Chen⁵

¹School of Petroleum Engineering, China University of Petroleum, Qingdao 266580, China

²Guizhou Panjiang Coalbed Methane Development and Utilization Company Limited, Guiyang 550081, China

³College of Resources and Environmental Engineering, Guizhou University, Guiyang 550025, China

⁴State Key Laboratory of Public Big Data, Guizhou University, Guiyang 550025, China

⁵The Electrical Engineering College, Guizhou University, Guiyang 550025, China

Correspondence should be addressed to Yuliang Su; suyuliang@upc.edu.cn

Received 8 June 2022; Revised 29 August 2022; Accepted 21 September 2022; Published 16 November 2022

Academic Editor: Basim Abu-Jdayil

Copyright © 2022 Yi Lou et al. This is an open access article distributed under the Creative Commons Attribution License, which permits unrestricted use, distribution, and reproduction in any medium, provided the original work is properly cited.

The coal facies and their effects on the coal pore characteristics of the Late Permian Longtan Formation, western Guizhou, were studied, using diverse experiments of macerals and minerals compositions, vitrinite reflectance, and pore characteristics. The results show that five coal facies exist in studied samples, and they are shallow-water covered forest peat swamp facies, moist forest peat swamp facies, dry forest peat swamp facies, low peat swamp facies, and wet land herbaceous peat swamp facies. Among them, the moist forest peat swamp facies accounts for the largest proportion, followed by the shallow-water covered forest peat swamp and dry forest peat swamp facies. The order of pore development degree is identical with the order of moist forest peat swamp facies coal > shallow-water covered forest peat swamp facies coal > dry forest peat swamp facies coal. In contrast to shallow-water covered forest peat swamp facies and dry forest peat swamp facies samples, moist forest peat swamp facies samples have higher porosity and larger pore size. Coal facies play an important role in controlling the pore structure of coal reservoir, which have more effect on pore size distribution than coal rank for the samples in this study.

1. Introduction

The implementation of China's "carbon emission peak and carbon neutrality" goals has resulted in unconventional natural gas being an important bridge for the transition from fossil fuels to new energy sources [1]. Coalbed methane, along with shale gas and tight gas, are the main components of unconventional natural gas known today [2]. However, unlike other unconventional natural gas, the development of coalbed methane not only provides clean energy but also safe and efficient mining of coal resources [3, 4].

In 2020, China's coalbed methane production reaches 6.7 billion cubic meters [5], strengthening our confidence in the development of the coalbed methane industry. The evaluation results of national coalbed methane resources

by the Strategic Research Center of the Ministry of Land and Resources show that the amount of coalbed methane geological resources in China is as high as 36 trillion cubic meters, of which 3.15 trillion cubic meters is located in Guizhou Province (accounting for about 10% of the country). Guizhou is thus the province of the most abundant coalbed methane resources in South China, and it is also the prospective province for the coalbed methane industry in China [6, 7].

Coal is a highly heterogeneous combustible organic rock composed of different macerals and minerals, and the macerals compositions, types, and distribution are controlled by the initial stage of coal formation, such as peat formation, diagenesis, and coalification [8–13]. The type and environment of bogs in the peatification stage are the main controlling factors for the composition and

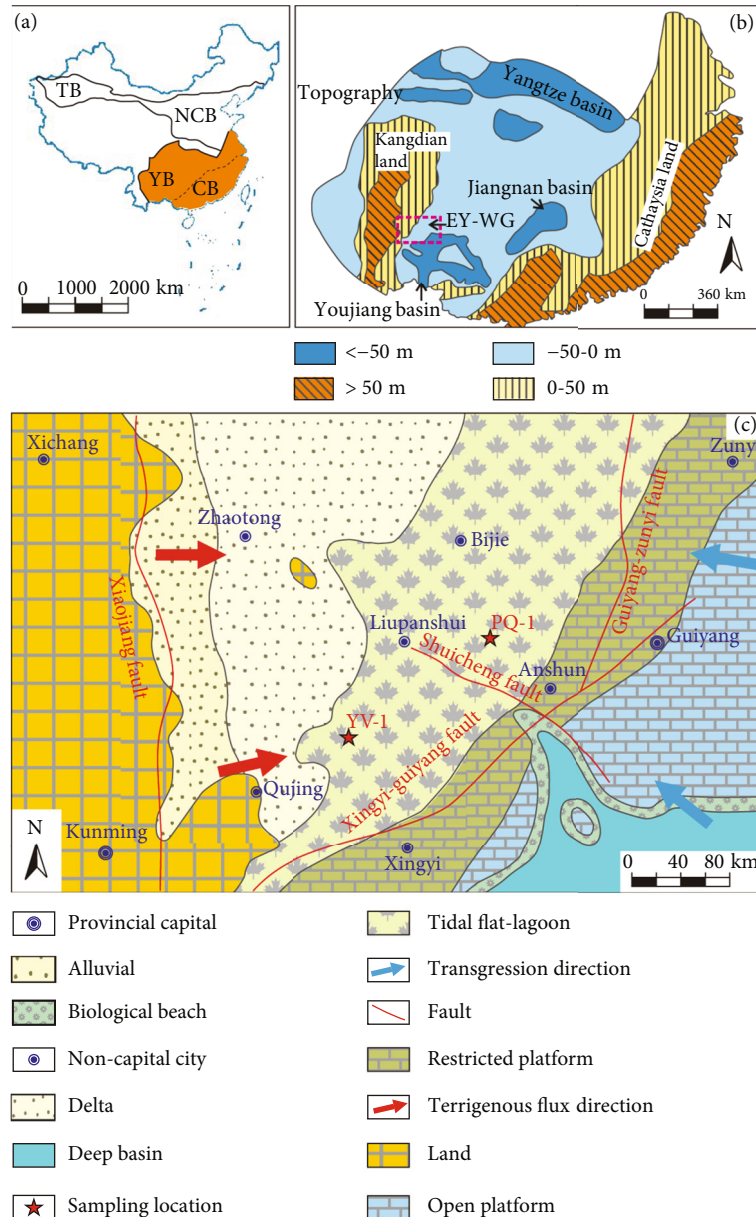


FIGURE 1: (a) Location of the South China block. (b) Tectonic characteristics of the South China block and the location of eastern Yunnan-western Guizhou area (based on [31, 40]). (c) Lithofacies paleogeography of eastern Yunnan-western Guizhou area (EY-WG) in the Late Permian (modified from [25, 26]) showing the sampling position of this study. TB: Tarim block; NCB: North China block; YB: Yangtze block; CB: Cathaysia block.

distribution of coal macerals [12, 14–15]. According to macerals compositions, coal facies can be subdivided into five types, and they are shallow-water covered forest peat moor, wetland herbaceous moor, shallow-water covered wetland herbaceous moor, moist forest peat moor, and low peat moor coal facies [13]. The composition and spatial distribution of coal macerals during peatification stage are important factors leading to interbedded, intrabedded, and planar heterogeneous of coal reservoirs, and coal facies has significant controls to reservoir pore structure [11, 16–22]. However, the effect of coal facies on pore characteristics of coal reservoirs and its mechanism are still unclear. The coal reservoirs of the Upper

Permian Longtan Formation in Guizhou Province have a complete range of coal ranks, and the effects of the thermal evolution on pore structure were analyzed [7, 23]. However, the research of coal facies for these coal reservoirs is inadequate.

In this study, we take the medium-rank coal and high-rank coal of the Longtan Formation in western Guizhou as research samples. Using the analyzing methods including macerals compositions, minerals compositions, vitrinite reflectance, and mercury intrusion porosimetry experiment, we divide the coal facies types, and then discussed the effect of coal facies on pore characteristics.

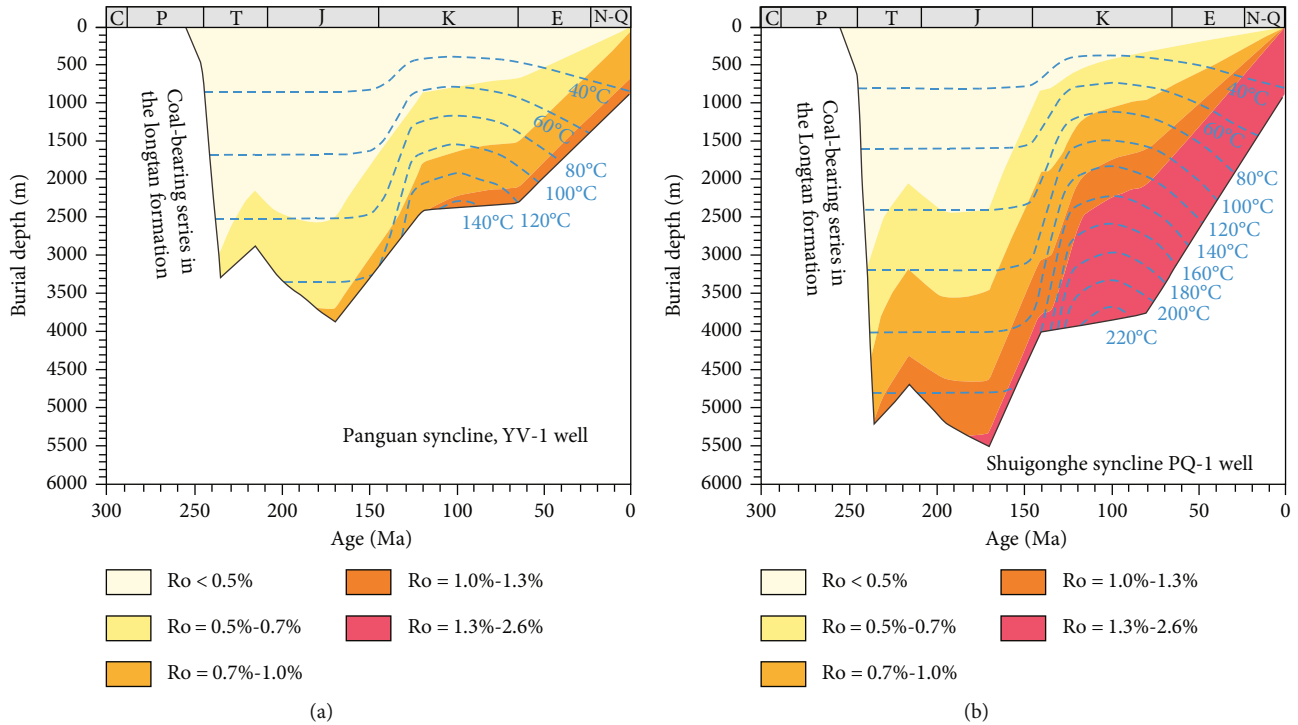


FIGURE 2: Burial history and thermal maturation process of coal seams in the Upper Permian Longtan formation. (a) Panguan syncline; (b) Shuigonghe syncline (modified from [23]).

2. Geological Background

The western Guizhou area is located at the southern edge of the Upper Yangtze block, mainly including the eastern part of the southwestern Guizhou Depression, eastern Yunnan-central Guizhou uplift, Qiannan Depression and southeastern Panjiang Depression, and this area was subjected to the joint action of the Tethys tectonic domain and the Pacific Coastal tectonic domain [24]. First, the deep-water sedimentary zone in the south was further deepened, expanded, and developed with volcanic clastic turbidites followed by the appearance of the terrestrial, maritime, and land interactions and marine phases from west to east (Figure 1) [25]. The marine intrusion during the Changxing stage of the Leping Period continued until the Middle Triassic. With the expansion of the marine intrusion, the terrestrial clastic deposits were gradually replaced by carbonate deposits [26]. The coal seam of the Longtan Formation in the western Guizhou region has experienced two stages of sedimentation and three phases of hydrocarbon generation, but there are obvious differences between the southwestern Panguan syncline and northeastern Shuigonghe syncline [23].

In the Panguan syncline, the first stage of sedimentary burial occurred in the Early–Middle Triassic, which was in a stable terrace stage and formed a giant thick shallow terrace-phase carbonate deposit. The second stage of sedimentary burial occurred in the Early–Middle Jurassic and formed a large terrestrial lake basin deposit, which reached 1200 m in thickness in this area (Figure 2(a)) [23]. The first phase of hydrocarbon generation occurred in the Early–Middle Triassic, with the paleo-temperature of the Longtan Formation reaching about 90°C at the end of the Middle Tri-

assic. The reflectivity (R_o) of the mirror group was about 0.6%, corresponding to the long-flame coal stage, and the primary biogenic gas and early thermogenic gas were dominant in this stage. The second phase of hydrocarbon generation occurred in the Middle Jurassic, with the paleo-temperature of the Longtan Formation reaching about 110°C at the end of the Middle Jurassic, exceeding the highest temperature of the previous stage, and the coal seam again. The third phase of hydrocarbon generation occurred in the Late Jurassic–Early Cretaceous, and under the influence of tectonic-thermal events, the paleo-geothermal gradient reached up to 5.5°C/100 m. The paleo-geothermal temperature of the Longtan Formation in the Panguan syncline rose sharply to about 140°C, with R_o value in 0.9%–1.2%, corresponding to the stage of fatty coal. During this phase, condensate began to cracking into methane, generating a large amount of thermogenic methane.

In the Shuigonghe syncline, the first stage of sedimentary burial occurred in the Early–Middle Triassic, depositing about 5200 m of the Middle and Lower Triassic (Figure 2(b)) [23]; the second stage of sedimentary burial occurred in the Early–Middle Jurassic, depositing about 1000 m of the Middle and Lower Jurassic. The first phase of hydrocarbon generation occurred in the Early–Middle Triassic. The paleo-geothermal temperature of the Longtan Formation is about 140–150°C at the end of the Middle Triassic, and the R_o value ranging from 1.0% to 1.2%. The second phase of hydrocarbon generation mainly occurred in the Middle Jurassic. The paleo-geothermal temperature of the Longtan Formation at the end of the Middle Jurassic was about 160°C, and R_o values are in 1.2%–1.5%, corresponding to the coking coal stage, producing a large amount

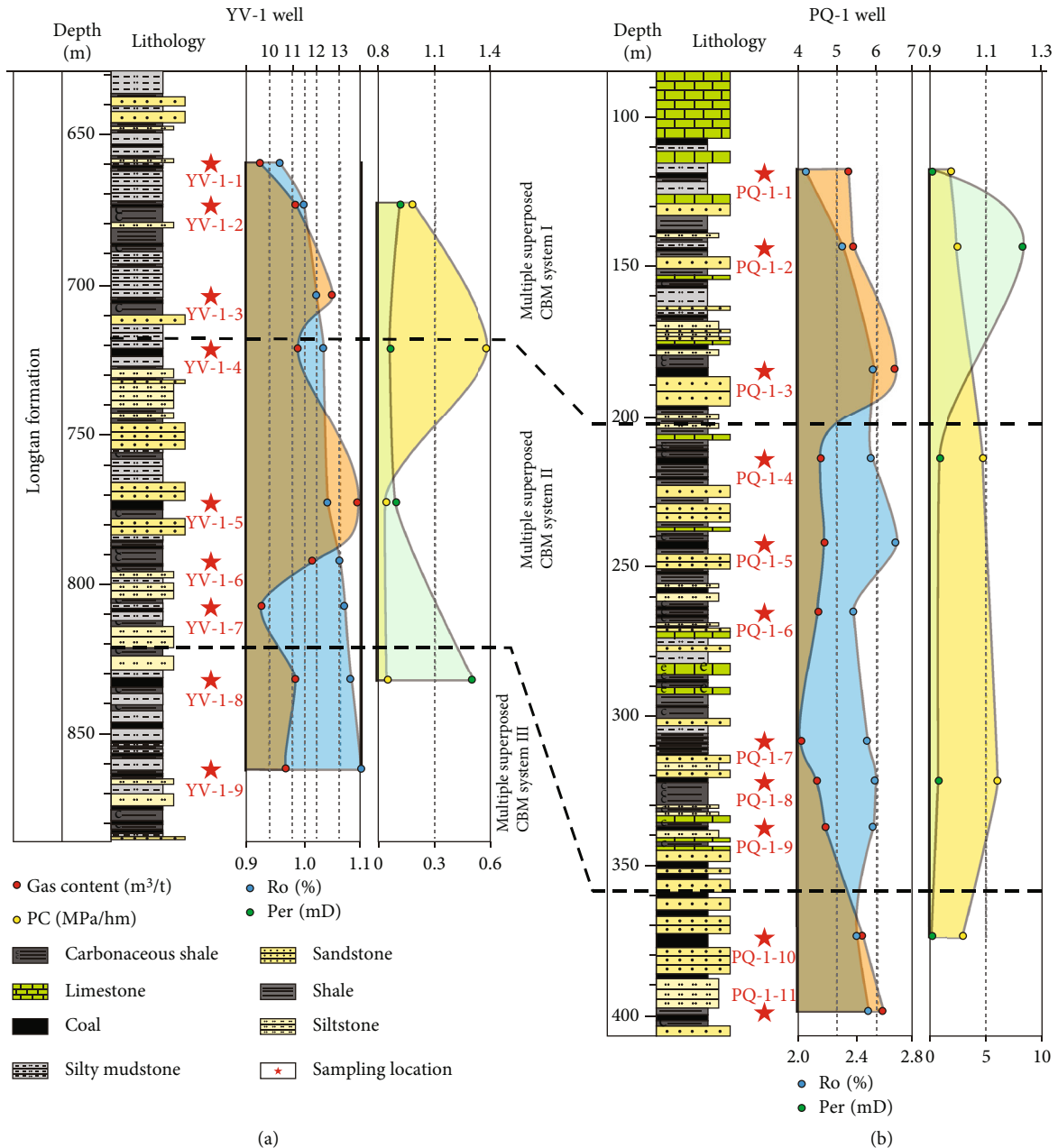


FIGURE 3: Sampling locations of wells PV-1 and PQ-1, showing the gas content, R_o , pressure coefficient, and permeability of samples. The division of multiple superposed CBM system was modified from [41].

of thermogenic methane gas. The third phase of hydrocarbon generation occurred in the Middle Yanshanian period. Owing to the tectonic-thermal events in the Early Cretaceous, the paleo-temperature of the Longtan Formation rise sharply to about 220°C with R_o values in 2.6%–3.5%, reaching the anthracite stage and producing a large amount of pyrogenic methane.

3. Materials and Methods

3.1. Sample Collection and Preparation. A total of 20 fresh coal samples were collected from two wells for the analyses conducted in this study. Eleven of them were from well PQ-

1 in the Shuigonghe syncline (Figure 3(a)), and the rest were from well YV-1 in the Panguan syncline (Figure 3(b)). These fresh coal samples were sealed using plastic wrap immediately, and then transported to laboratory, and then were processed to powdered, thin slice, cylinder samples in the Laboratory of Coal Geology Bureau of Guizhou Province.

3.2. Analytical Methods. In this study, the macerals compositions, minerals compositions, and vitrinite reflectance (R_o) of 20 coal samples were analyzed to determine their petrological characteristics. Based on these analyzing results, coal facies parameters were calculated to divide coal facies of these coal samples. Mercury intrusion porosimetry

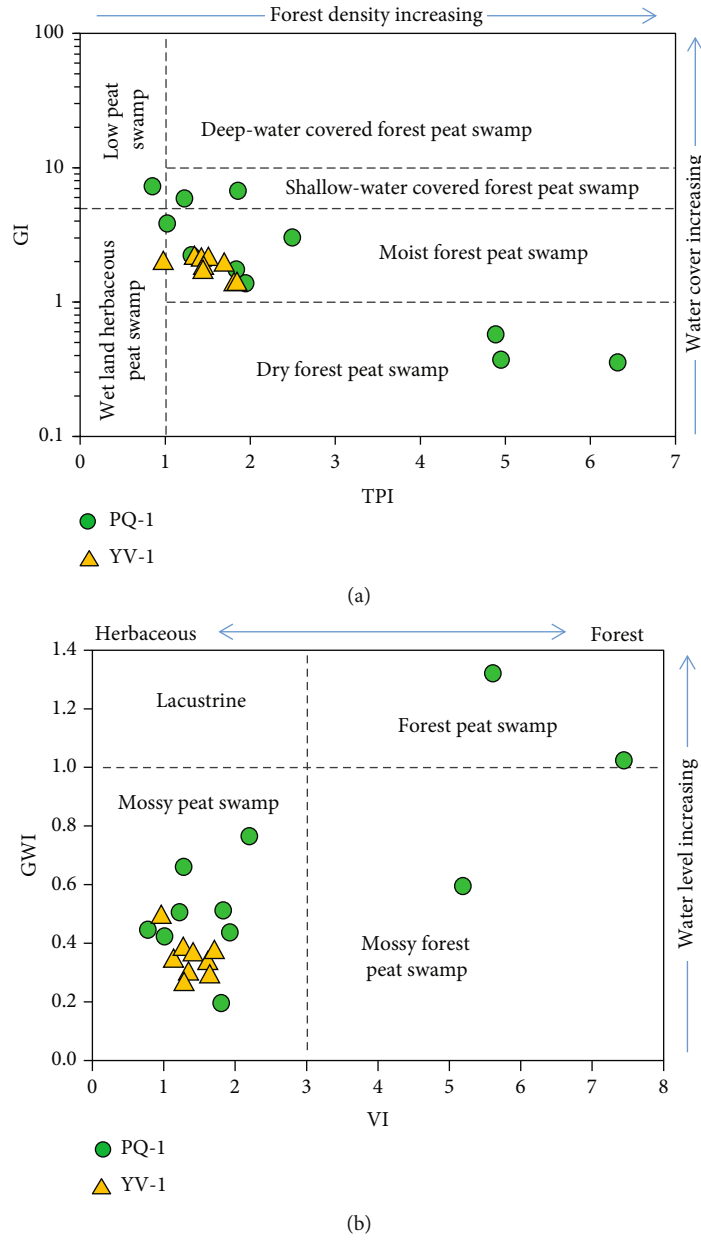


FIGURE 4: GI-TPI cross-plot (a) (modified from [28]) and GWI-VI cross-plot (b) (modified from [30]) for identifying coal facies.

experiment was conducted to determine the pore features of these coal samples, including porosity, pore size distribution, and pore connectivity. All these experiments were conducted in the Laboratory of Coal Geology Bureau of Guizhou Province.

The mercury intrusion porosimetry experiment was conducted using a Poremaster 60GT automatic mercury porosimeter following the China Petroleum and Natural Gas Industry Standard (SY/T 5346-2005). The equilibration time was set as 10 s, and evacuation time was 5 mins during experiments. Compared with the gas adsorption method, a more comprehensive range of pore sizes could be measured with mercury intrusion porosimetry, including pore characteristics of mesopore and macropore that cannot be measured by the gas adsorption method. During the MIP

experiment, pressure of mercury injection increases with decreasing pore size. Pore radiuses were calculated using the Washburn equation [27] as follows:

$$r_{\max} 2\sigma \cos \theta / P_T, \tag{1}$$

where P_T is mercury injection pressure, MPa; σ is surface tension, set to be 0.48 N/m; θ is the contact angle between mercury and coal, set to be 141 degree; r_{\max} is the maximum capillary radius, μm .

In addition to the experiments above, gas content, reservoir pressure, and permeability of well testing were collected from the Guizhou Panjiang Coalbed Methane Development and Utilization Company Limited.

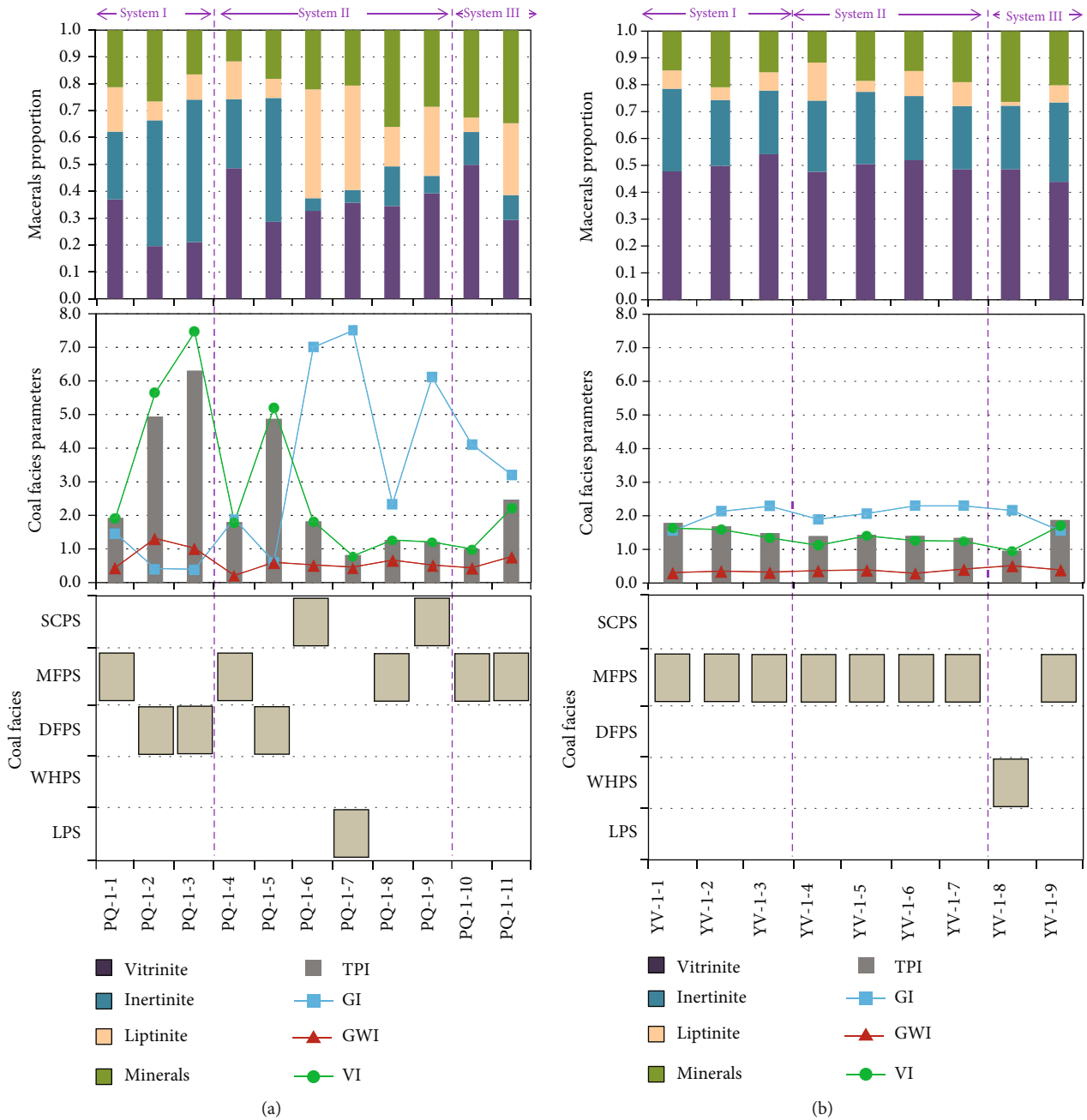


FIGURE 5: Columnar sequences of coal facies and its corresponding parameters of studied coal samples. (a) PQ-1 well; (b) YV-1 well.

4. Results and Discussion

4.1. Coal Facies Identification. Coal facies could be identified using coal facies parameters, including Texture Preservation Index (TPI), Gelification Index (GI), Groundwater Index (GWI), and Vegetation Index (VI) [11–13, 19, 28, 29]. The TPI refers the degradation intensity of plant tissue and the preservation degree of plant cells of coal forming plants, and can also be used to reflect the change of pH value. The GI is the ratio of gelation components to nongelatinization components, reflecting the wettability

and duration of peat bog during the process of peat accumulation. Based on GI-TPI diagram, coal facies can be divided into land, piedmont, arid forest swamp, upper delta plain, humid forest swamp, lake, and lower delta plain [28]. GWI-VI diagram is another prevalent method to evaluate coal facies [29, 30]. The GWI is based on gelation and mineral input, representing the water level during the formation of peat bog. The VI is the ratio of the components retaining the cell structure to the matrix, clastic material and granular components, reflecting the type of coal forming vegetation and its preservation degree. In this

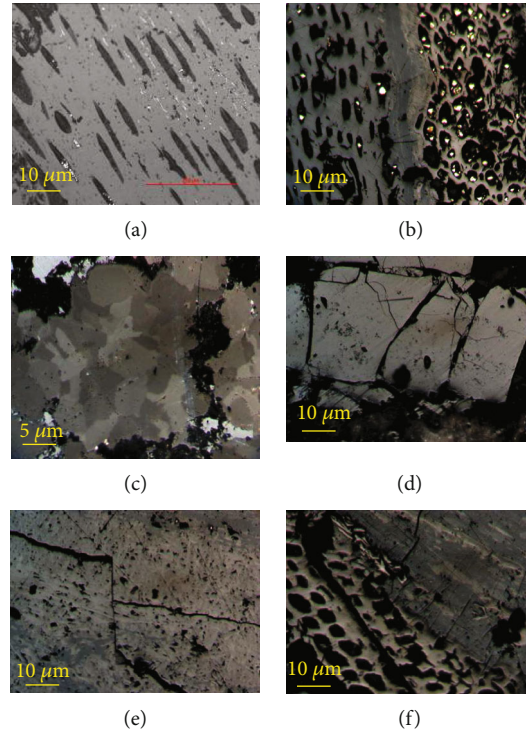


FIGURE 6: Microphotographs of macerals. (a) Cavity pores in fusinite; (b) cavity pores in telinite and fusinite; (c) intergranular pores among mineral particles; (d) cleats in telocollinite; (e) fractures in fusinite; (f) cavity pores and fractures in telinite and fusinite.

study, based on macerals compositions, the TPI, GI, GWI, and VI were calculated by the formula [28, 29] given as follows:

$$\text{TPI} = \frac{(\text{Telinite} + \text{Telocollinite} + \text{Fusinite} + \text{Semifusinite})}{(\text{Desmocollinite} + \text{Vitrodetrinite} + \text{Gelocollinite} + \text{Corpocollinite} + \text{Inertodetrinite} + \text{Macrinite}),}$$

$$\text{GI} = \frac{(\text{Vitrinite} + \text{Macrinite})}{(\text{Fusinite} + \text{Semifusinite} + \text{Inertodetrinite})}$$

$$\text{GWI} = \frac{(\text{Vitrodetrinite} + \text{Gelocollinite} + \text{Corpocollinite} + \text{Minerals})}{(\text{Telinite} + \text{Telocollinite} + \text{Desmocollinite}),}$$

$$\text{VI} = \frac{(\text{Telinite} + \text{Telocollinite} + \text{Corpocollinite} + \text{Fusinite} + \text{Semifusinite} + \text{Resinite} + \text{Suberinite})}{(\text{Desmocollinite} + \text{Vitrodetrinite} + \text{Inertodetrinite} + \text{Liptodetrinite} + \text{Sporinite} + \text{Cutinite}).} \quad (2)$$

The GI-TPI cross-plot of studied coal samples was shown in Figure 4(a). The TPI and GI of the coal samples from PQ-1 well range in 0.82–6.31 (averaging 2.58) and 0.40–7.50 (averaging 3.19), respectively. In contrast to PQ-1 well, the coal samples from YV-1 well have lower and concentrated TPI (varying from 0.96 to 1.88, with an average of 1.49) and GI (varying from 1.56 to 2.30, with an average of 2.03) values. In the GI-TPI cross-plot

(Figure 4(a)), the coals from PQ-1 well basically fall in shallow-water covered forest swamp facies, moist forest swamp facies, and dry forest swamp facies, and only one sample (sample PQ-1-7) fall in low swamp facies. YV-1 coal samples mainly fall in moist forest swamp facies, and only one sample (sample YV-1-8) fall in wet land herbaceous swamp facies.

The GWI values of coals from PQ-1 well range from 0.07 to 0.45, implying that the gelation degree and minerals input content of different coal seams in this well are highly variable. Compared with PQ-1 well, the samples from YV-1 well have lower and much concentrated GWI values (0.1–0.23) (Figure 4(b)), indicating that these samples have weak gelation degree and minerals input. The VI of the samples from PQ-1 well and YV-1 well are 0.79–7.45 and 0.96–1.70, with the average values of 2.76 and 1.36, respectively. This result indicates that the coal-forming plants at YV-1 are mainly herbaceous plants, while the coal-forming plants at PQ-1 are herbaceous and woody.

Combined with GI-TPI and GWI-VI, the coal facies of studied samples were divided into shallow-water covered forest peat swamp facies, moist forest peat swamp facies, dry forest peat swamp facies, low peat swamp facies, and wet land herbaceous peat swamp facies.

4.2. Coal-Forming Environment. The location of YV-1 well was closer to the Kangdian land, which is the main provenance of the eastern Yunnan-western Guizhou area, than the location of PQ-1 well, even though both of them are distributed in tidal flat-lagoon environment during the Late Permian (Figure 1) [26, 31]. During the sedimentation of

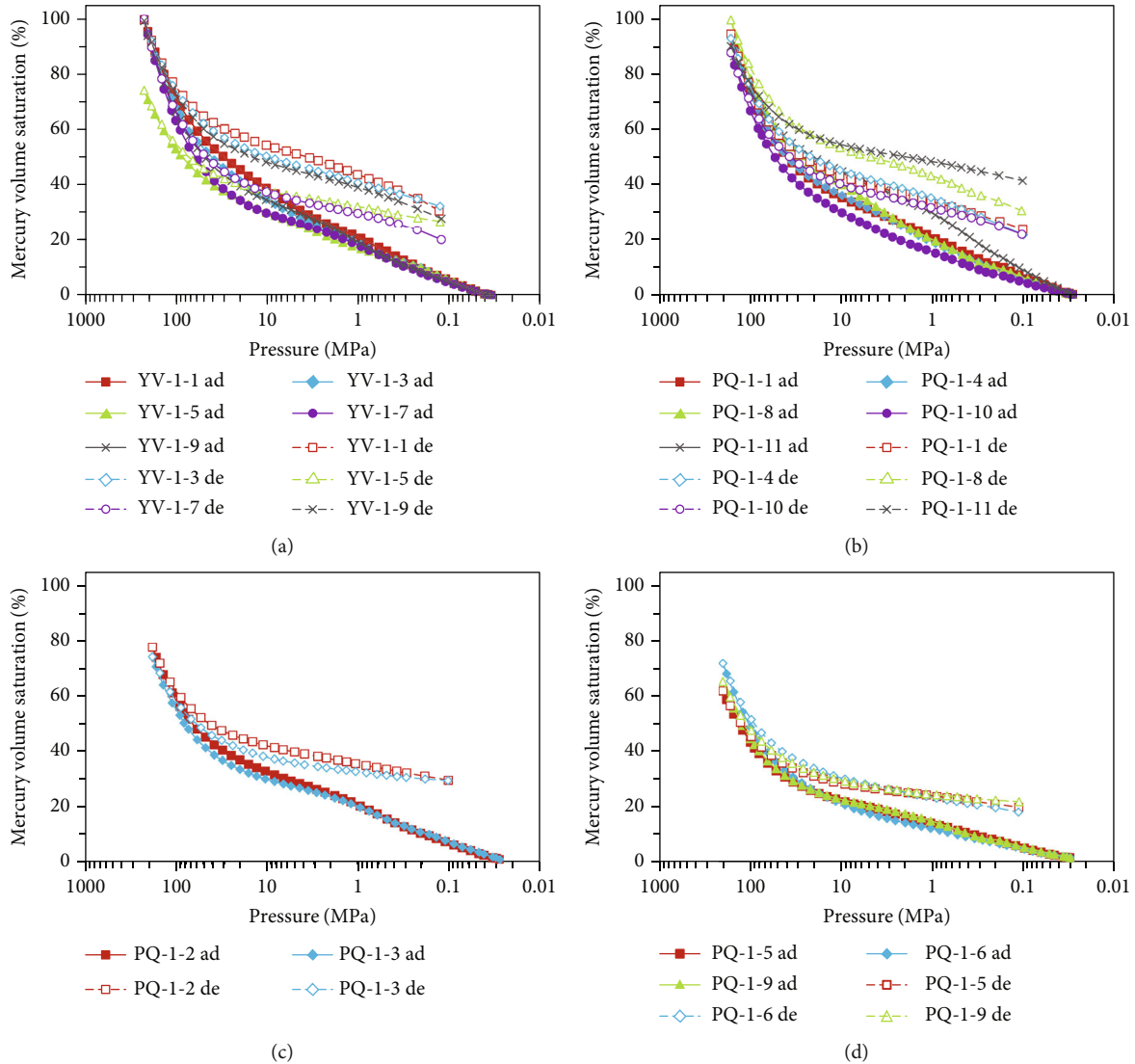


FIGURE 7: Mercury injection (ad) and withdrawal curves (de) of different coal facies. (a) Moist forest peat swamp facies of YV-1 well; (b) moist forest peat swamp facies of PQ-1 well; (c) shallow-water covered forest peat swamp facies of PQ-1 well; and (d) dry forest peat swamp facies of PQ-1 well.

the Longtan coal-bearing formation, the location of PQ-1 well has deeper water and less terrigenous input than that of YV-1 well [25]. As a result, PQ-1 well lithology includes limestone, sandstone, siltstone, shale, and coal, while there is no limestone in YV-1 well lithology (Figure 3). These differences between YV-1 well and PQ-1 well imply that coal-forming peat swamps are heterogeneous in studied areas during the sedimentation of the Longtan coal-bearing formation.

Based on coal facies parameters, five peat swamp facies were recognized among studied coal samples from the Longtan coal-bearing formation. In YV-1 well, the coals were mainly formed in moist forest peat swamp, and only one sample (YV-1-8) was formed in wet land herbaceous peat swamp (Figure 5(b)), indicating a relatively stable coal-forming environment. A possible reason is that the terrigenous input rate offsets the effect of transgression, and then

maintains a relatively stable water depth and forest density at the location of YV-1 well during the sedimentation of the Longtan coal-bearing formation. During this period, however, both the water depth and forest density at the location of PQ-1 well were unstable, and the coals in this well mainly formed in shallow-water covered forest peat swamp facies, moist forest peat swamp facies, and dry forest peat swamp (Figure 5(a)). We deduce that this unstable environment is controlled by transgression. The evidence is that both shallow-water covered forest peat swamp facies samples (PQ-1-6 and PQ-1-9) are surrounded by limestone (Figure 3(b)). In addition, coals from YV-1 well have much less difference in macerals proportion compared with those coals from PQ-1 well (Figures 5(a) and 5(b)), also implying that the location of YV-1 well had more stable environment than the location of PQ-1 well during the sedimentation of the Longtan coal-bearing formation.

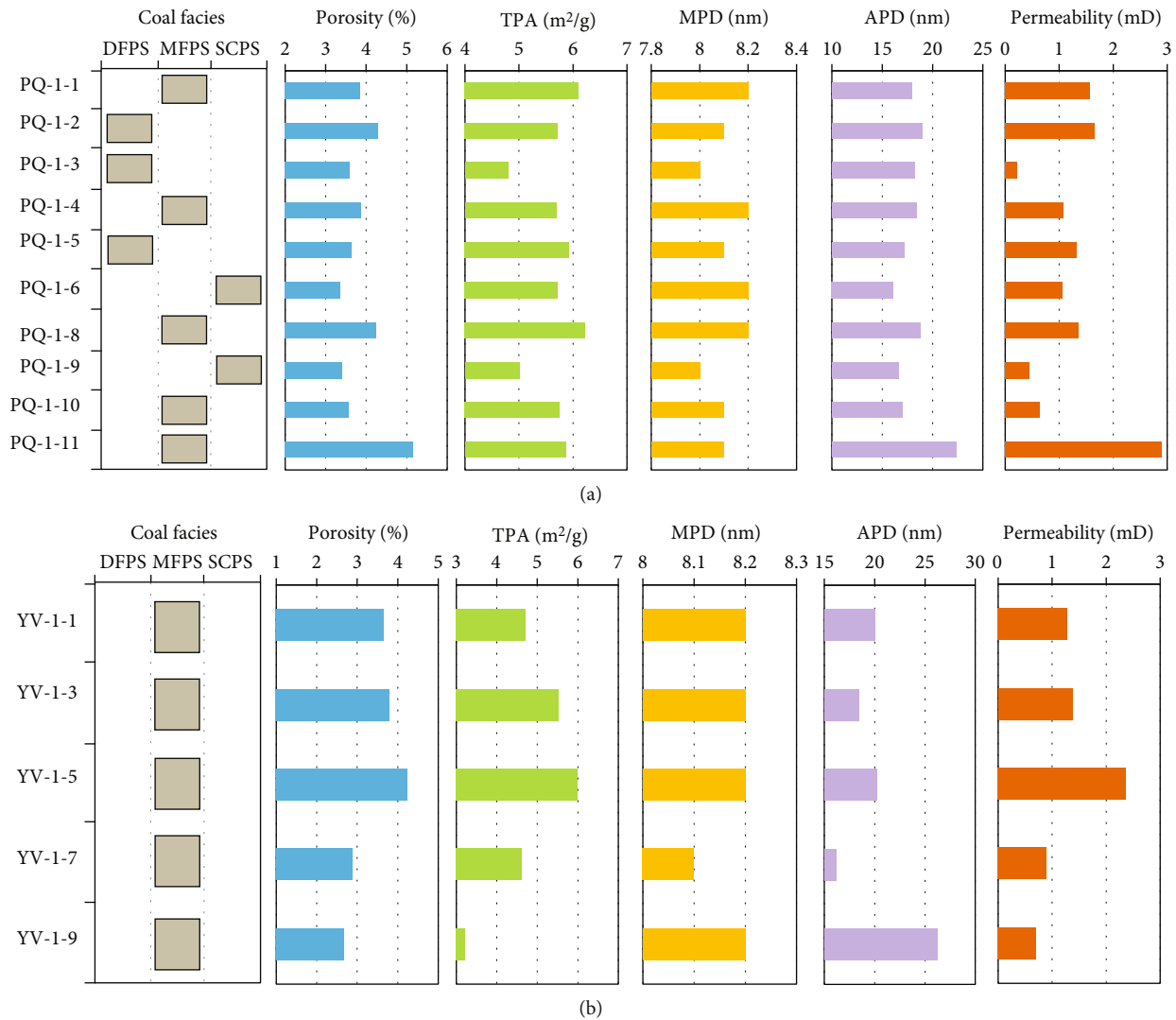


FIGURE 8: Porosity, total pore area (TPA), median pore diameter (MPD), average pore diameter (APD), and permeability of moist forest peat swamp facies (MFPS), shallow-water covered forest peat swamp facies (SCPS), and dry forest peat swamp facies (DFPS) samples based on mercury intrusion porosimetry experiment data. (a) PQ-1 well; (b) YV-1 well.

4.3. Pore Characteristics of Various Coal Facies. The paleo-environment governs the degree and feature of pore development by affecting the coal lithotype and macerals composition [8, 9, 12, 13, 16, 32], and some macerals are porous (Figure 6). Previous studies indicate that there is close connection between coal facies parameters and different sizes pores of medium-rank coal [10, 19], while there are no data to support the correlation of high-rank coal and the dual control from coal facies and coal rank to pore structure. In this study, mercury intrusion porosimetry experiment was conducted to recognize the pore features of various coal facies and coal ranks. As shown in Figure 7, moist forest peat swamp facies samples have much higher mercury volume saturation than shallow-water covered forest peat swamp facies samples and dry forest peat swamp facies samples, implying that the degree of pore development follows the following order: moist forest peat swamp facies coal > shallow-water covered forest peat swamp facies coal > dry forest peat swamp facies coal.

Based on mercury intrusion porosimetry experiment data, the porosity, total pore area (TPA), median pore diameter (MPD), average pore diameter (APD), and permeability were calculated, and the results are shown in Figure 8. Considering samples from PQ-1 well, which are high-rank coals with R_o of 2.05%–2.69% (Figure 3), the porosity, TPA, MPD, and APD of shallow-water covered forest peat swamp facies samples range in 3.35%–3.41%, 5.01–5.72 m²/g, 8–8.2 nm, and 16.1–16.6 nm, respectively. They are 3.60%–4.29%, 4.80–5.93 m²/g, 8–8.1 nm, and 17.2–19 nm, respectively, in dry forest peat swamp facies samples. In contrast to the shallow-water covered forest peat swamp facies and dry forest peat swamp facies samples, moist forest peat swamp facies samples have higher porosity and larger pore sizes. Their porosity, TPA, MPD, and APD, range in 3.56%–5.16%, 5.69–6.22 m²/g, 8.1–8.2 nm, and 17–22.3 nm, respectively (Figure 8(a)). As shown in Table 1, among these three coal facies, moist forest peat swamp facies have the highest average porosity, TPA, permeability, MPD, and APD. It is

TABLE 1: Average porosity, surface area, permeability, median pore diameter, and average pore diameter of various coal facies based on mercury intrusion porosimetry experiment data.

Parameters	MFPS (YV-1 well)	MFPS (PQ-1 well)	DFPS (PQ-1 well)	SCPS (PQ-1 well)
Porosity (%)	3.44	4.14	3.84	3.38
Total pore area (m^2/g)	4.81	5.92	5.49	5.36
Permeability (mD)	1.33	1.50	1.06	0.75
Median pore diameter (nm)	8.18	8.16	8.07	8.10
Average pore diameter (nm)	20.20	18.88	18.13	16.35

Note: MFPS: moist forest peat swamp facies; SCPS: shallow-water covered forest peat swamp facies; and DFPS: dry forest peat swamp facies.

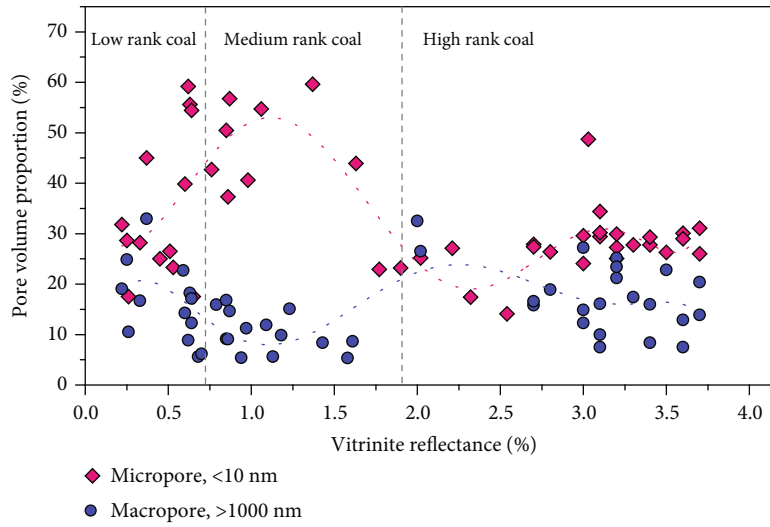


FIGURE 9: Relationship between vitrinite reflectance and pore volume of different kinds of pores (the data is cited from references [33–37]).

noteworthy that moist forest peat swamp facies samples from YV-1 well, which are medium-rank coal with R_o of 0.95%–1.1%, have poorer porosity (2.66%–4.22%) and TPA (3.23–5.98 m^2/g) and slightly larger MPD (8.1–8.2 nm) and APD (16.2–26.2 nm) than the same coal facies samples from PQ-1 well. This result is consistent with former researchers, and they indicated that micropores proportion reach peak during 0.75%–1.25% R_o stage, while the peak of macropores occurs during 2.0%–2.5% R_o stage (Figure 9) [33–38].

As shown in Figure 10, coal samples have significant heterogeneity in pore size distribution, and different kinds of pores including macropores (>1000 nm), mesopores (100–1000 nm), transition pores (10–100 nm), and micropores (<10 nm) have different correlations with various coal facies parameters. We recognized that (1) the TPI has a weak negative correlation with mesopores but a positive correlation with macropores, and no significant correlation with micropores and transition pores (Figures 10(a)–(d)); (2) the GI is positively correlated with micropores and transition pores, negatively correlated with mesopores and macropores (Figures 10(e)–(h)); (3) the GWI is negatively correlated with micropores and transition pores, and positively correlated with macropores (Figures 10(i)–(l)); and (4) the VI has a weak negative correlation with transition pores and mesopores, and a weak positive correlation with macropores (Figures 10(m)–(p)). These results indicate that coal facies

play an important role in controlling the pore structure of coal reservoir. By combining macroscopic coal facies with microscopic pore structure and establishing multiscale coal reservoir model, the reservoir properties can be characterized more accurately.

When comparing the average pore size distribution of moist forest peat swamp facies samples from high-rank coal (PQ-1 well) and medium-rank coal (YV-1 well), we found that there is no significant difference between them (Figure 11). The coal facies has much stronger control on pore size distribution than coal rank for the samples in this study.

4.4. Applications of Coal Facies in CBM Industry for Guizhou Province. Coal facies have significant effects on pore structure in coal reservoirs [10, 11, 13, 19, 39]. Coal facies are determined by sedimentary environment of coal reservoirs, and are the bridge between sedimentary environment and reservoirs properties [12, 15]. Recognizing the heterogeneous distribution of coal facies is important to reservoirs evaluation. Especially in Guizhou Province, where the coal reservoirs are multilayer thin coal seams [7]. In addition, previous studies have proved that coal rank is another controlling factor to reservoir properties (Figures 9 and 12) [33–37], and coal rank reflects tectonic evolution of coal reservoir. Generally, medium rank coal has much higher

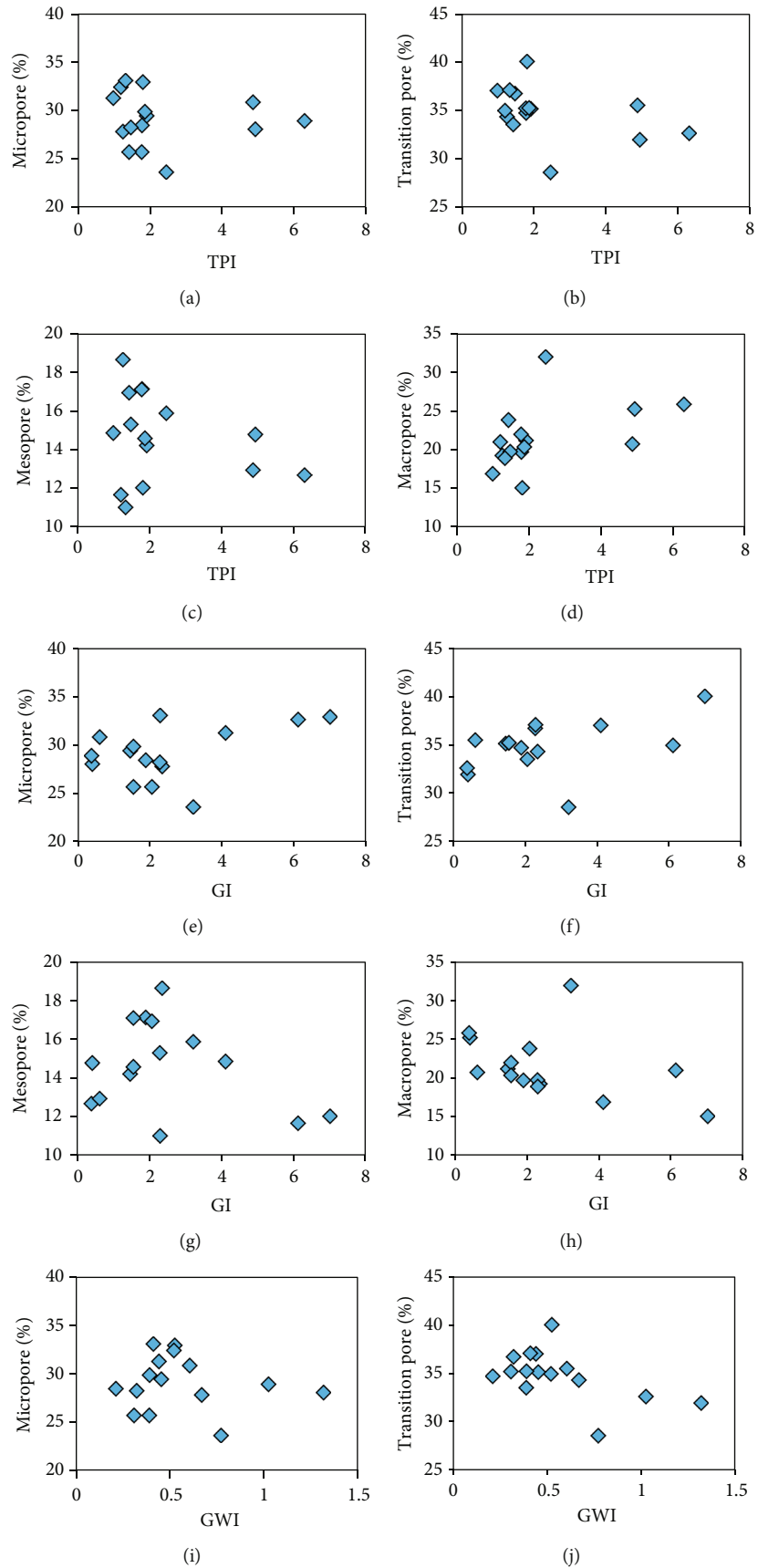


FIGURE 10: Continued.

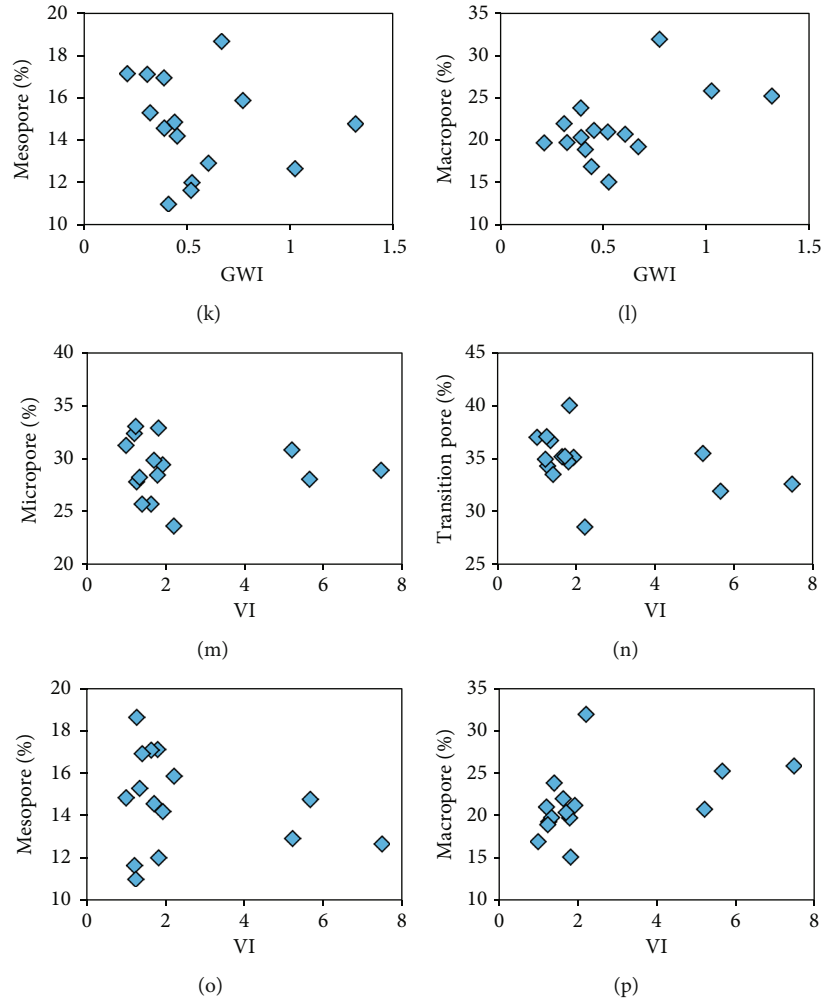


FIGURE 10: Relationships between the pore size and coal facies parameters. (a) Micropores (<10 nm) versus TPI; (b) transition pores (10-100 nm) versus TPI; (c) mesopores (100-1000 nm) versus TPI; (d) macropores (>1000 nm) versus TPI; (e) Micropores versus GI; (f) transition pores versus GI; (g) mesopores versus GI; (h) macropores versus GI; (i) micropores versus GWI; (j) transition pores versus GWI; (k) mesopores versus GWI; (l) macropores versus GWI; (m) micropores versus VI; (n) transition pores versus VI; (o) mesopores versus VI; (p) macropores versus VI.

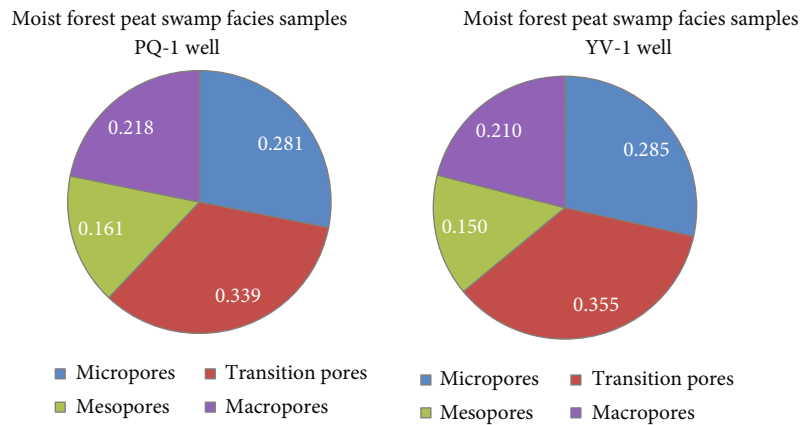


FIGURE 11: Average pore size proportion of moist forest peat swamp facies samples from PQ-1 and YV-1 wells.

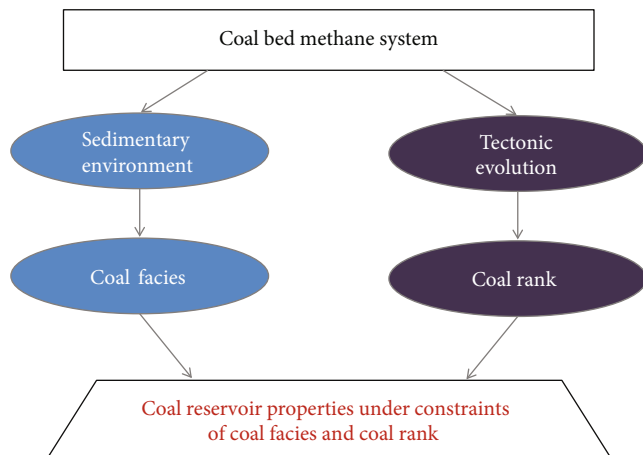


FIGURE 12: Relationship among sedimentary environment, tectonic evolution, coal facies, coal rank, and reservoir properties.

proportion of micropores and lower proportion of macropores than low and high rank coals. However, the experimental results in this study show that a same coal facies (MFPS) from PQ-1 well (high rank coal samples, Figure 3(b)) and YV-1 well (medium rank coal samples, Figure 3(a)), samples from PQ-1 well have lower median pore diameter and average pore diameter, but higher total pore area than those samples from YV-1 (Table 1). Moreover, SCPS coal facies samples from PQ-1 well have lower average pore diameter and total pore area than both MFPS and DFPS coal facies samples even though they are all high rank coal samples (Table 1). These results implying that coal facies plays more important role affecting pore structure than coal ranks for the Longtan Formation coals in western Guizhou area.

Combining macroscopic coal facies (related to coal reservoir sedimentary environment) and coal rank (related to coal reservoir tectonic evolution), the study of microscopic pore structure characteristics of different coal phase and coal grade of coal reservoirs will provide a new theoretical basis for coalbed methane exploration and development in Guizhou Province.

5. Conclusions

Twenty coal samples of the Longtan formation were collected from PQ-1 and YV-1 wells in western Guizhou, to analyze the coal facies and their effects on pore characteristics. Three conclusions have been obtained.

- (1) Based on coal facies parameters including TPI, GI, GWI, and VI, the coal facies of studied samples were divided into shallow-water covered forest peat swamp facies, moist forest peat swamp facies, dry forest peat swamp facies, low peat swamp facies, and wet land herbaceous peat swamp facies. The coals samples from YV-1 well were mainly formed in moist forest peat swamp, and only one sample (YV-1-8) was formed in wet land herbaceous peat swamp. The coal samples from PQ-1 well mainly

formed in shallow-water covered forest peat swamp facies, moist forest peat swamp facies, and dry forest peat swamp

- (2) Pore development degree follows a descending order, namely moist forest peat swamp facies coal, shallow-water covered forest peat swamp facies coal, dry forest peat swamp facies coal. In contrast to the samples of shallow-water covered forest peat swamp facies and dry forest peat swamp facies, moist forest peat swamp facies samples have higher porosity and larger pore size
- (3) Coal facies plays more important role affecting pore structure than coal ranks for the Longtan Formation coals in western Guizhou area

Data Availability

The data used to support the findings of this study are available from the corresponding author upon request.

Conflicts of Interest

The authors declare that they have no conflicts of interest.

Acknowledgments

This work was financially supported by the Qian Science Cooperation Project of Prospecting Strategy (Grant No. [2022] ZD001), the Project from Guizhou Panjiang Coalbed Methane Development and Utilization Company Limited (Grant No. p2022011), the Guizhou Provincial Fund Project (Grant Nos. [2020]1Y161 and ZK [2022] YIBAN106), and the Geological Exploration Fund Project of Guizhou Province (Grant No. 52000021MGQSE7S7K6PRP).

References

- [1] C. N. Zou, Q. Zhao, L. Z. Cong et al., "Development progress, potential and prospect of shale gas in China," *Natural Gas Industry*, vol. 41, no. 1, pp. 1–12, 2021.
- [2] Z. J. Jin, J. C. Zhang, and X. Tang, "Unconventional natural gas accumulation system," *Natural Gas Industry*, vol. 41, no. 8, pp. 58–68, 2021.
- [3] T. A. Moore, "Coalbed methane: a review," *International Journal of Coal Geology*, vol. 101, no. 1, pp. 36–81, 2012.
- [4] Y. Qin, J. G. Wu, G. Z. Li et al., "Patterns and pilot project demonstration of coal measures gas production," *Journal of China Coal Society*, vol. 45, no. 7, pp. 2513–2522, 2020.
- [5] Department of Petroleum and Natural Gas and National Energy Administration, Institute of Resources and Environmental Policy, development research center of the State Council, oil and gas resources strategy research center, Ministry of Natural Resources, *China Natural Gas Development Report 2021*, Petroleum Industry Press, 2021.
- [6] Y. Qin and D. Gao, *Prediction and evaluation of coalbed methane resource potential in Guizhou Province*, China University of Mining and Technology Press, 2012.

- [7] J. Jin, Z. B. Yang, Y. Qin et al., “Progress, potential and prospects of CBM development in Guizhou Province,” *Journal of China Coal Society*, vol. 46, pp. 1–13, 2021.
- [8] C. R. Clarkson and R. M. Bustin, “Variation in permeability with lithotype and maceral composition of Cretaceous coals of the Canadian Cordillera,” *International Journal of Coal Geology*, vol. 33, no. 2, pp. 135–151, 1997.
- [9] M. Mastalerz, A. Drobniak, and J. Rupp, “Meso- and micro-pore characteristics of coal lithotypes: implications for CO₂ adsorption,” *Energy & Fuels*, vol. 22, no. 6, pp. 4049–4061, 2008.
- [10] S. Zhang, S. Tang, D. Tang, Z. Pan, and F. Yang, “The characteristics of coal reservoir pores and coal facies in Liulin district, Hedong coal field of China,” *International Journal of Coal Geology*, vol. 81, no. 2, pp. 117–127, 2010.
- [11] L. Zhao, Y. Qin, C. F. Cai et al., “Control of coal facies to adsorption-desorption divergence of coals: a case from the Xiqu drainage area, Gujiao CBM Block, North China,” *International Journal of Coal Geology*, vol. 171, no. 15, pp. 169–184, 2017.
- [12] B. Jiu, W. H. Huang, and R. L. Hao, “A method for judging depositional environment of coal reservoir based on coal facies parameters and rare earth element parameters,” *Journal of Petroleum Science and Engineering*, vol. 207, article 109128, 2021.
- [13] Y. Q. Zhai, *The Characteristics of Coal Facies in the Permian Coal Seams in the North of Pingdingshan and Its Control of Coal Pore Characteristics*, Henan University of Technology, 2020.
- [14] M. B. Silva, W. Kalkreuth, and M. Holz, “Coal petrology of coal seams from the Leao-Butia Coalfield, Lower Permian of the Parana Basin, Brazil – Implications for coal facies interpretations,” *International Journal of Coal Geology*, vol. 73, no. 3–4, pp. 331–358, 2008.
- [15] J. Li, X. G. Zhuang, and J. B. Zhou, “Coal facies characteristic and identification of transgressive/regressive coal-bearing cycles in a thick coal seam of Xishanyao formation in eastern Junggar coalfield, Xinjiang,” *Journal of Jilin University*, vol. 42, pp. 104–114, 2012.
- [16] Y. D. Cai, D. M. Liu, Z. J. Pan, Y. B. Yao, J. Q. Li, and Y. K. Qiu, “Pore structure and its impact on CH₄ adsorption capacity and flow capability of bituminous and subbituminous coals from Northeast China,” *Fuel*, vol. 103, pp. 258–268, 2013.
- [17] T. Li, C. F. Wu, and Q. Liu, “Characteristics of coal fractures and the influence of coal facies on coalbed methane productivity in the South Yanchuan Block, China,” *Journal of Natural Gas Science and Engineering*, vol. 22, pp. 625–632, 2015.
- [18] J. Lu, L. Y. Shao, M. F. Yang et al., “Depositional model for peat swamp and coal facies evolution using sedimentology, coal macerals, geochemistry and sequence stratigraphy,” *Journal of Earth Science*, vol. 28, no. 6, pp. 1163–1177, 2017.
- [19] Y. J. Lu, D. M. Liu, Y. D. Cai, Q. Li, and Q. F. Jia, “Pore-fractures of coalbed methane reservoir restricted by coal facies in Sangjiang-Muling coal-bearing basins, Northeast China,” *Energies*, vol. 13, no. 5, p. 1196, 2020.
- [20] M. Li, B. Jiang, Q. Miao, G. Wang, Z. J. You, and F. J. Lan, “Multi-phase tectonic movements and their controls on coalbed methane: a case study of no. 9 coal seam from eastern Yunnan, SW China,” *Energies*, vol. 13, no. 22, article 6003, 2020.
- [21] Z. G. Zhang, Q. Qin, Z. J. You, and Z. B. Yang, “Distribution characteristics of in situ stress field and vertical development unit division of CBM in Western Guizhou, China,” *Natural Resources Research*, vol. 30, no. 5, pp. 3659–3671, 2021.
- [22] Z. G. Zhang, Y. Qin, T. S. Yi, Z. J. You, and Z. B. Yang, “Pore structure characteristics of coal and their geological controlling factors in eastern Yunnan and Western Guizhou, China,” *ACS Omega*, vol. 5, no. 31, pp. 19565–19578, 2020.
- [23] Z. X. Dou, *Tectonic Evolution and Its Control on Coalbed Methane Reservoiring in Western Guizhou*, China University of Mining, 2012.
- [24] Guizhou Geological Survey Institute, *Regional Geology of China-Guizhou Chronicle*, Geological Press, 2017.
- [25] L. Y. Zhao, P. M. Zhou, Y. Lou et al., “Geochemical characteristics and sedimentary environment of the upper Permian Longtan coal series shale in Western Guizhou Province, South China,” *Geofluids*, vol. 2021, Article ID 9755861, 11 pages, 2021.
- [26] X. T. Wang, L. Y. Shao, K. A. Eriksson et al., “Evolution of a plume-influenced source-to-sink system: an example from the coupled Central Emeishan large igneous province and adjacent western Yangtze cratonic basin in the late Permian, SW China,” *Earth-Science Reviews*, vol. 207, pp. 103–223, 2019.
- [27] Y. D. Cai, D. M. Liu, Y. F. Zhou, and D. W. Lv, “Insights into matrix compressibility of coals by mercury intrusion porosimetry and N₂ adsorption,” *International Journal of Coal Geology*, vol. 200, no. 1, pp. 199–212, 2018.
- [28] C. F. K. Diessel, “On the correlation between coal facies and depositional environments,” *The University of Newcastle, Newcastle*, vol. 6, pp. 19–22, 1986.
- [29] J. H. Calder, M. R. Gibling, and P. K. Mukhopadhyay, “Peat formation in a Westphalian B piedmont setting, Cumberland Basin, Nova Scotia; implications for the maceral-based interpretation of rheotrophic and raised paleomires,” *Bulletin de la Société Géologique de France*, vol. 168, no. 2, pp. 283–298, 1991.
- [30] C. F. K. Diessel, *Coal-Bearing Depositional System*, Springer-Verlag, Berlin Heidelberg, 1992.
- [31] S. Z. Shen, Y. Wang, C. M. Henderson, C. Q. Cao, and W. Wang, “Biostratigraphy and lithofacies of the Permian System in the Laibin-Heshan area of Guangxi, South China,” *Palaeoworld*, vol. 16, no. 1–3, pp. 120–139, 2007.
- [32] A. Busch and Y. Gensterblum, “CBM and CO₂-ECBM related sorption processes in coal: a review,” *International Journal of Coal Geology*, vol. 87, no. 2, pp. 49–71, 2011.
- [33] L. Chen, L. Zhang, Q. J. Kang, H. S. Viswanathan, J. Yao, and W. Q. Tao, “Nanoscale simulation of shale transport properties using the lattice Boltzmann method: permeability and diffusivity,” *Scientific Reports*, vol. 5, pp. 2045–2322, 2015.
- [34] Z. Q. Ouyang, D. M. Liu, Y. D. Liu, and Y. B. Yao, “Fractal analysis on heterogeneity of pore-fractures in middle-high rank coals with NMR,” *Energy & Fuels*, vol. 30, no. 7, pp. 5449–5458, 2016.
- [35] Y. L. Liu, D. Z. Tang, H. Xu, S. Li, and S. Tao, “The impact of coal macrolithotype on hydraulic fracture initiation and propagation in coal seams,” *Journal of Natural Gas Science and Engineering*, vol. 56, pp. 299–314, 2018.
- [36] B. Y. Wang, Y. Qin, J. Shen, Q. S. Zhang, and G. Wang, “Pore structure characteristics of low- and medium-rank coals and their differential adsorption and desorption effects,” *Journal of Petroleum Science and Engineering*, vol. 165, pp. 1–12, 2018.

- [37] Q. Zhu, Y. Yang, X. Lu et al., “Pore structure of coals by mercury intrusion, N₂ adsorption and NMR: a comparative study,” *Applied Sciences*, vol. 9, no. 8, p. 1680, 2019.
- [38] Q. Luo, L. Zhang, N. Zhong et al., “Thermal evolution behavior of the organic matter and a ray of light on the origin of vitrinite-like maceral in the Mesoproterozoic and lower Cambrian black shales: insights from artificial maturation,” *International Journal of Coal Geology*, vol. 244, article ???, 2021.
- [39] D. M. Liu, Q. F. Jia, and Y. D. Cai, “Research progress on coalbed methane reservoir geology and characterization technology in China,” *Coal Science and Technology*, vol. 50, no. 1, pp. 196–203, 2022.
- [40] Y. Wang and J. Yugan, “Permian palaeogeographic evolution of the Jiangnan Basin, South China,” *Palaeogeography, Palaeoclimatology, Palaeoecology*, vol. 160, no. 1-2, pp. 35–44, 2000.
- [41] Y. L. Shen, Y. Qin, Y. H. Guo, T. S. Yi, Y. B. Shao, and H. B. Jin, “Sedimentary controlling factor of unattached multiple superimposed coalbed-methane system formation,” *Earth Science-Journal of China University of Geosciences*, vol. 37, no. 3, pp. 573–579, 2012.